



HAL
open science

A five-transgene cassette confers broad-spectrum resistance to a fungal rust pathogen in wheat

Ming Luo, Liqiong Xie, Soma Chakraborty, Aihua Wang, Oadi Matny, Michelle Jugovich, James A Kolmer, Terese Richardson, Dhara Bhatt, Mohammad Hoque, et al.

► To cite this version:

Ming Luo, Liqiong Xie, Soma Chakraborty, Aihua Wang, Oadi Matny, et al.. A five-transgene cassette confers broad-spectrum resistance to a fungal rust pathogen in wheat. *Nature Biotechnology*, 2021, 39, pp.561 - 566. 10.1038/s41587-020-00770-x . hal-03906159

HAL Id: hal-03906159

<https://hal.inrae.fr/hal-03906159>

Submitted on 19 Dec 2022

HAL is a multi-disciplinary open access archive for the deposit and dissemination of scientific research documents, whether they are published or not. The documents may come from teaching and research institutions in France or abroad, or from public or private research centers.

L'archive ouverte pluridisciplinaire **HAL**, est destinée au dépôt et à la diffusion de documents scientifiques de niveau recherche, publiés ou non, émanant des établissements d'enseignement et de recherche français ou étrangers, des laboratoires publics ou privés.



Distributed under a Creative Commons Attribution 4.0 International License



A five-transgene cassette confers broad-spectrum resistance to a fungal rust pathogen in wheat

Ming Luo¹, Liqiong Xie², Soma Chakraborty¹, Aihua Wang¹, Oadi Matny³, Michelle Jugovich³, James A. Kolmer⁴, Terese Richardson¹, Dhara Bhatt¹, Mohammad Hoque¹, Mehran Patpour⁵, Chris Sørensen⁶, Diana Ortiz⁶, Peter Dodds¹, Burkhard Steuernagel⁷, Brande B. H. Wulff⁷, Narayana M. Upadhyaya¹, Rohit Mago¹, Sambasivam Periyannan¹, Evans Lagudah¹, Roger Freedman⁸, T. Lynne Reuber^{8,9}, Brian J. Steffenson³ and Michael Ayliffe¹✉

Breeding wheat with durable resistance to the fungal pathogen *Puccinia graminis* f. sp. *tritici* (*Pgt*), a major threat to cereal production, is challenging due to the rapid evolution of pathogen virulence. Increased durability and broad-spectrum resistance can be achieved by introducing more than one resistance gene, but combining numerous unlinked genes by breeding is laborious. Here we generate polygenic *Pgt* resistance by introducing a transgene cassette of five resistance genes into bread wheat as a single locus and show that at least four of the five genes are functional. These wheat lines are resistant to aggressive and highly virulent *Pgt* isolates from around the world and show very high levels of resistance in the field. The simple monogenic inheritance of this multigene locus greatly simplifies its use in breeding. However, a new *Pgt* isolate with virulence to several genes at this locus suggests gene stacks will need strategic deployment to maintain their effectiveness.

Pgt continues to overcome resistant wheat cultivars, with three new, highly virulent isolates emerging in the last 20 years, and the disease reappearing in Europe and the UK¹. Two classes of *Pgt* resistance genes have been cloned from wheat: all-stage resistance (ASR) genes and adult plant resistance (APR) genes². ASR genes (for example, *Sr22* (ref. ³), *Sr35* (ref. ⁴), *Sr45* (ref. ³) and *Sr50* (ref. ⁵)) generally encode nucleotide-binding, leucine-rich repeat (NLR) proteins that recognize a specific *Pgt* molecule (an effector) introduced into host plant cells by the fungus to promote parasitism, whereupon a plant defense response is activated². The presence, absence or allelic variation of the fungal effector determines which *Pgt* isolates an ASR gene is effective against. ASR genes are extremely valuable for crop protection but, when deployed singly, often show transient resistance, as pathogen effectors rapidly evolve to avoid recognition. Combining ASR genes increases their durability, and theoretical estimates suggest that the chance of a single *Pgt* isolate gaining virulence for five or more ASR genes in wheat is infinitesimally small⁶.

The second gene class, APR genes, can be remarkably durable and, in some cases, effective against multiple pathogen species. However, these genes generally provide partial resistance that is often insufficient for crop protection during severe pathogen epidemics.

For example, the gene known as *Sr55*, *Lr67*, *Yr46* or *Pm46* (hereafter *Sr55*) provides partial APR to all tested isolates of *Pgt*, *Puccinia triticina* (*Pt*, wheat leaf rust pathogen), *Puccinia striiformis* f. sp. *tritici* (*Pst*, wheat stripe rust pathogen) and *Blumeria graminis* f. sp. *tritici* (wheat powdery mildew pathogen). *Sr55* encodes a defective hexose transporter protein that provides resistance by an unknown mechanism⁷. The current paradigm for durable resistance posits that multiple ASR genes fortified by APR genes provide the most durable resistance. Herein we have introduced a transgene cassette of four ASR genes (*Sr22*, *Sr35*, *Sr45* and *Sr50*), combined with the APR gene *Sr55*, into bread wheat as a single locus.

A major obstacle in producing polygenic resistance gene stacks is the generally large size of each gene. We generated a 37-kb transfer (T)-DNA construct encoding *Sr22*, *Sr35*, *Sr45*, *Sr50* and *Sr55* and including endogenous 5' and 3' regulatory sequences of these genes (Fig. 1a), by developing a reiterative Gateway recombinase cloning strategy that uses excisable *lacZ* selection for large-construct generation (Fig. 1b). This highly effective cloning strategy is independent of restriction enzyme site availability or sequence domestication and is described in detail in Supplementary Fig. 1a–d. Using this strategy, we have generated resistance gene T-DNA inserts in sizes exceeding 60 kb.

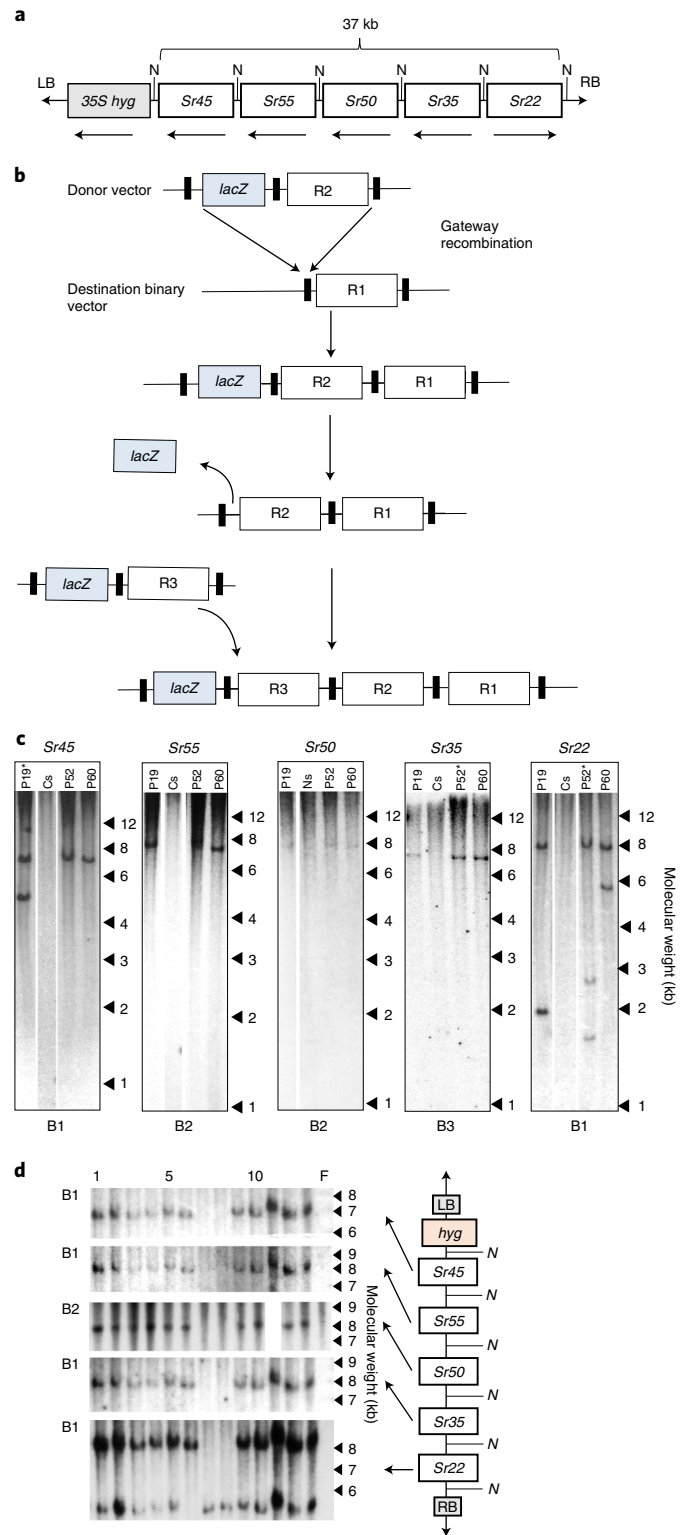
We then introduced the *Sr22*–*Sr35*–*Sr45*–*Sr50*–*Sr55* cassette into bread wheat cultivar Fielder by *Agrobacterium*-mediated transformation. Of the 80 T₀ plants produced, five had all sequence junctions between adjacent resistance genes and vector sequences, based on PCR amplification. Three of these plants (P19, P52, P60) contained all five genes as full-length NotI restriction fragments as shown using DNA blot analysis and gene-specific probes (Fig. 1c), while two plants were missing one full-length gene (Supplementary Table 1). In the T₁ progeny of P19, P52 and P60, all five full-length genes were inherited as a single locus in each family (Fig. 1d, Supplementary Table 2 and Supplementary Figs. 2–4), confirming the co-insertion of each gene. However, some additional partial transgene fragments were also present in each line, most commonly for the *Sr22* gene, adjacent to the T-DNA right border sequence (Supplementary Table 1 and Fig. 1c,d). In some, but not all instances, these partial fragments were co-inherited with the full-length gene locus (Supplementary Figs. 2–4).

¹CSIRO Agriculture and Food, GPO Box 1700, Canberra, Australia. ²School of Life Science and Technology, Xinjiang University, Urumqi, China. ³Department of Plant Pathology, Stakman-Borlaug Center for Sustainable Plant Health, University of Minnesota, St. Paul, MN, USA. ⁴USDA-ARS Cereal Disease Laboratory, St. Paul, MN, USA. ⁵Department of Agroecology, Aarhus University, Slagelse, Denmark. ⁶Genetics and Breeding of Fruit and Vegetables Unit, National Research Institute for Agriculture, Food and Environment, Montfavet, France. ⁷John Innes Centre, Norwich Research Park, Norwich, UK. ⁸2Blades Foundation, Evanston, IL, USA. ⁹Present address: Enko Chem, Woburn, MA, USA. ✉e-mail: michael.ayliffe@csiro.au

Fig. 1 | Generating transgenic Fielder wheat lines containing a multi-transgene resistance gene cassette. **a**, Multi-transgene cassette structure. The direction of transcription of each gene is indicated by arrows underneath. As part of the cloning strategy, each gene is flanked by NotI restriction enzyme sites (N). A hygromycin phosphotransferase selectable marker gene (*hyg*) under the regulatory control of a cauliflower mosaic virus 35S promoter was used for transgenic plant selection. LB, left border; RB, right border. **b**, Multi-transgene stack cloning strategy. Resistance genes, including their introns and 5' and 3' endogenous regulatory sequences, were cloned into a donor vector with a *lacZ* reporter gene adjacent to the cloning site. Both genes were then introduced into a destination binary vector by Gateway recombination; recombination sites are shown as solid black rectangles. *lacZ*-positive *Escherichia coli* colonies were selected, and *lacZ* was excised from the plasmid by Gateway recombination to re-establish a destination vector containing two resistance genes. The process was then reiterated to sequentially add additional genes. Details of this procedure are given in Supplementary Fig. 1a–d and the Methods. **c**, DNA blot analysis of multi-transgene T_0 plants P19, P52 and P60. DNA was digested with the restriction enzyme NotI and hybridized with the gene-specific sequences indicated above each blot. Three independent DNA blots derived from the same genomic DNA samples (B1–B3) were hybridized. Lane C contains DNA from a Fielder control line, while lane N contains DNA from a Fielder line null for this transgene. Arrowheads on the right indicate molecular weight in kb. Bands approximately 8 kb in size encode full-length genes, while other smaller bands are partial sequence integrants. (*A 1-kb band with homology to the *Sr35* probe and a 4-kb band with homology to *Sr22* can also be observed in P52 in some instances, while a faint 5.5-kb band with homology to *Sr45* can be seen in the P19 sample upon longer exposure (Supplementary Figs. 2 and 3 and Supplementary Table 1)). **d**, Segregation analysis of T_1 progeny from the multi-transgene line P60. DNA was digested with the restriction enzyme NotI and hybridized with the gene-specific probes indicated on the right. Lanes in each image are derived from the same genomic DNA samples but were hybridized with different probes. Two independent DNA blots using the same genomic DNA (B1 and B2) were hybridized. The lane labeled 'F' contains nontransgenic Fielder control DNA. A more extensive segregation analysis can be seen in Supplementary Figs. 2–4. Arrowheads indicate molecular weight in kb. Note that sample 11 is missing in the third image.

We then tested homozygous progeny from these three lines for *Pgt* resistance using glasshouse seedling assays and field trials. T_2 seedlings from each line were infected with seven diverse *Pgt* isolates that were virulent toward up to 17 of 20 differential wheat lines carrying single endogenous *Sr* genes (Supplementary Table 3). Fielder and null controls were highly susceptible to six of these seven isolates. In contrast, all multi-transgene seedlings were highly resistant to all *Pgt* isolates (infection type (IT) 0), including the isolate JRCQC (increased resistance, avirulent toward Fielder) (Supplementary Figs. 5–11). Fielder transgenic plants containing *Sr22* were also resistant to all isolates, although with slightly increased pathogen sporulation (Supplementary Table 3, IT 1). As expected, multi-transgenic and Fielder seedlings were equally susceptible to *Pst* and *Pt* (Supplementary Table 3).

Homozygous T_5 multi-transgene lines were also extremely resistant to *Pgt* race QTHJC in two independent field trials undertaken in 2018 and 2019, where only hypersensitive flecks developed with no pathogen sporulation (Fig. 2a,b; average disease severity (ADS), 0%). In contrast, susceptible control lines LMPG-6 and Morocco (ADS, 73–100%) and Fielder and null-segregant controls (ADS, 53–96%) were very heavily infected (Fig. 2a,b and Supplementary Table 4). Single-gene transgenic lines with *Sr22* or *Sr50* were also resistant in the field but exhibited some pathogen sporulation (ADS, 1–17%), whereas lines with *Sr45* were susceptible to race QTHJC



(ADS, 55–91%) (Fig. 2a,b and Supplementary Table 4), as were lines with *Sr35*, although single-gene *Sr35* lines were tested in glasshouse assays only (Supplementary Figure 11 and Supplementary Table 3).

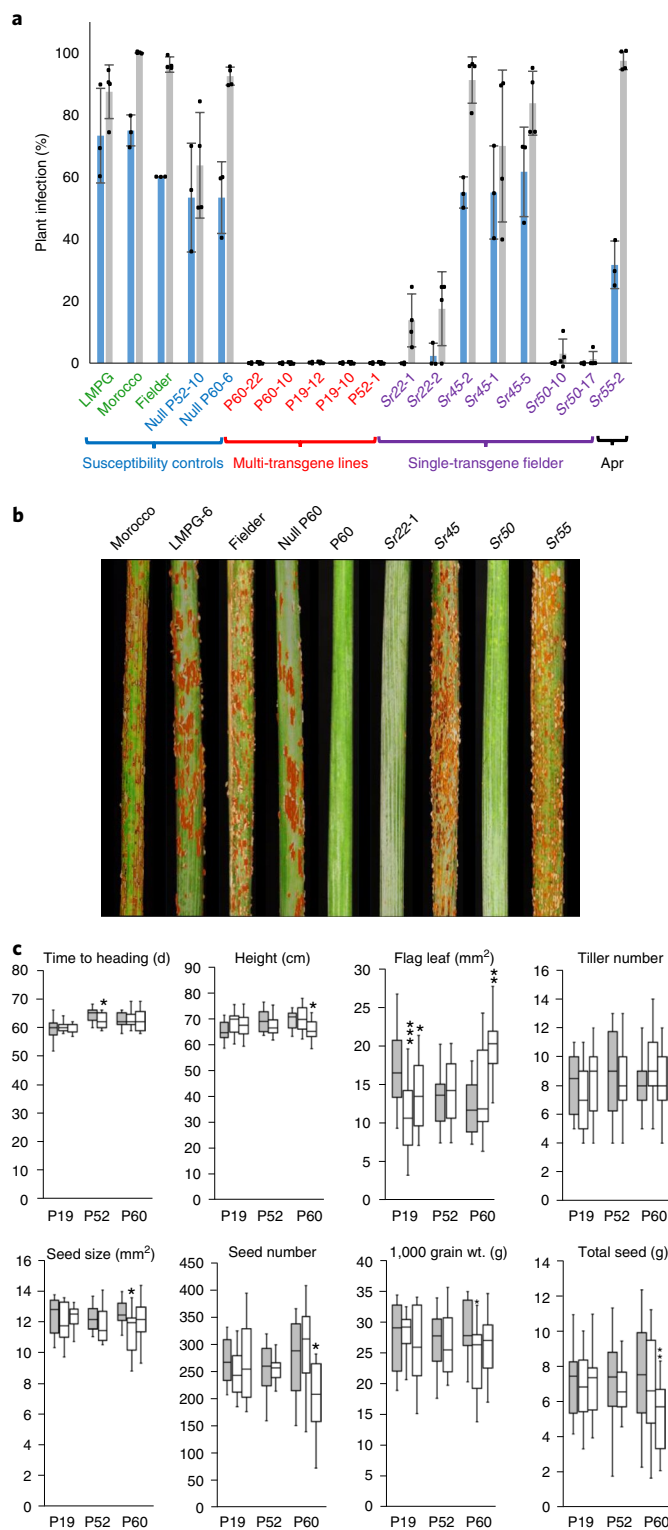
To determine whether these high levels of resistance were associated with pleiotropic effects arising from transgene expression, we conducted a greenhouse experiment in which multiple growth, development and yield parameters were assessed (Fig. 2c). Homozygous P52 and P60 multi-transgene lines were compared with their respective null-segregant lines, whereas line P19 was

Fig. 2 | Multi-transgene lines are highly resistant to *Pgt* without evidence of pleiotropic effects.

a, Stem rust field trial results of multi-transgene wheat lines in 2018 and 2019. Plants were artificially inoculated on three separate occasions with *Pgt* isolate QTHJC while growing to maturity. Each column shows the percent ADS of each line at the late dough stage with ADS calculated from three replicate plots in 2018 and four replicate plots in 2019. Data are shown as mean \pm s.d. The disease severity score for each replicate plot is illustrated as a black dot on each column. Data from the 2018 season are shown in blue, while results from 2019 are in gray (see also Supplementary Table 4). Homozygous T_5 families of multi-transgene lines are labeled in red, while homozygous transgenic Fielder lines containing a single resistance transgene are shown in purple. Nontransgenic susceptible wheat cultivars and multi-transgene null-segregant sibling lines are labeled green and blue, respectively. Statistical comparisons (one-sided ANOVA and post hoc Dunnett's test) of transgenic lines and Fielder and null controls are shown in Supplementary Table 4. **b**, Stem rust infection on flag leaf sheaths of selected multi-transgene (P60) and single-transgene lines, Fielder wild type and susceptible Morocco and LMPG-6 controls. Samples were infected with *Pgt* race QTHJC in the field in 2018, using three replicate plots per genotype. **c**, Comparison of selected growth, development and yield parameters of five homozygous multi-transgene lines (white boxes) versus controls (gray boxes) grown in the greenhouse. Box and whisker plots show data from 20 replicate plants per genotype from a single experiment. The boxed area encompasses the 25th to 75th percentile, with the median value indicated as a horizontal line, while whiskers define the smallest and largest quartiles. The measured phenotypic parameter is shown above each graph. A single multi-transgene line of P52 was compared with its null sibling control, and two homozygous P60 lines were compared with a P60 null sibling control. P19 lines were compared with a Fielder control. Statistical significance was determined by one-sided ANOVA and a post hoc Dunnett test for comparing means between multi-transgene lines and their respective controls. Statistically significant differences between a multi-transgene phenotype and its respective control are indicated as follows: * $P < 0.05$, ** $P < 0.01$, *** $P < 0.001$. Exact P values are shown in Supplementary Table 5.

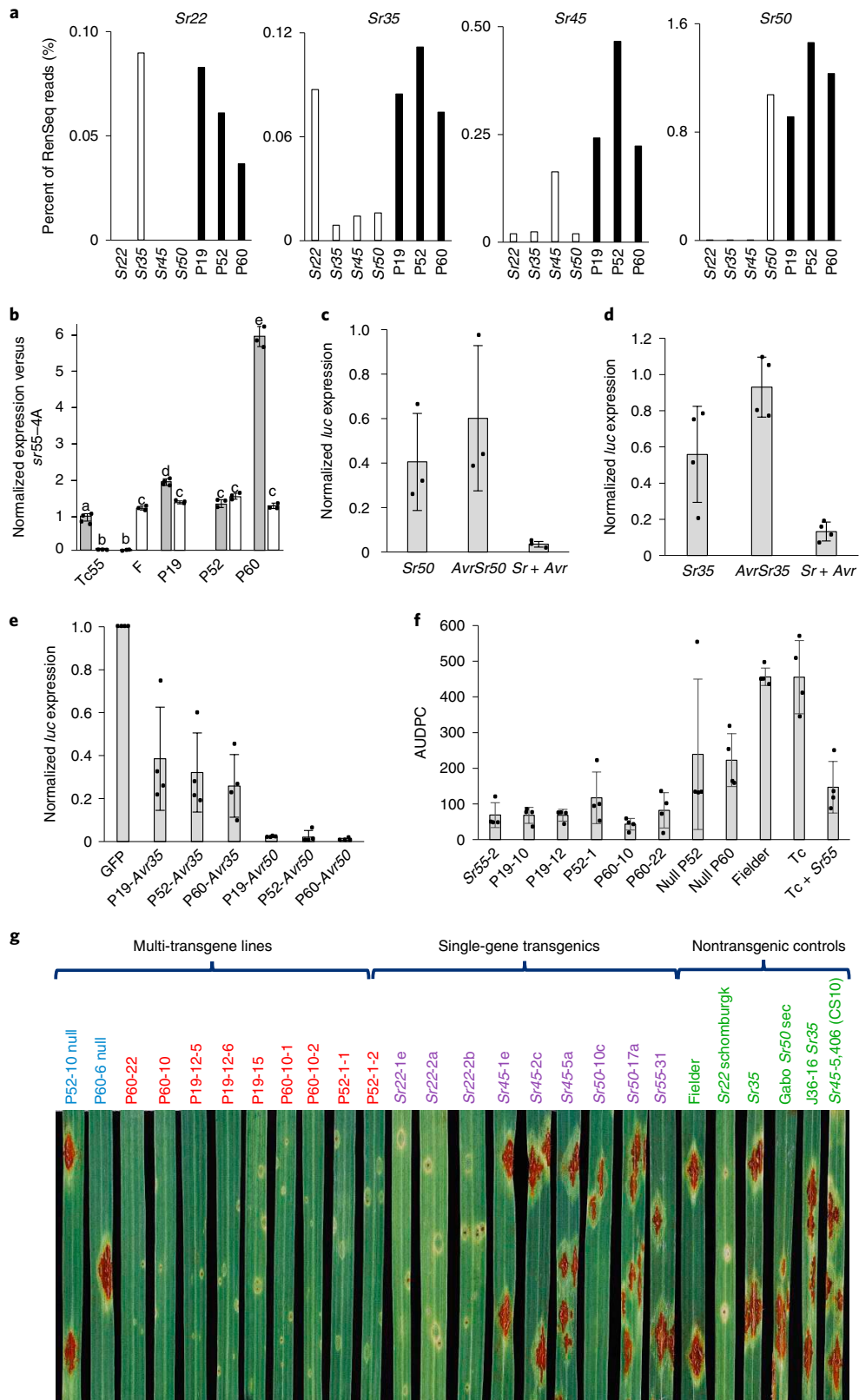
compared with Fielder due to the low seed availability of P19 null siblings. No consistent phenotypic differences were found between the multi-transgene and control lines (Fig. 2c and Supplementary Table 5). Similarly, we saw no obvious pleiotropic growth effects in multi-transgene lines in the two disease field trials. However, extensive multi-year and multi-environment field trialing in the absence of pathogen infection is required to confirm this observation.

While these data show that each multi-transgene line was highly resistant to *Pgt*, they do not confirm function of each gene at the locus. Using resistance gene enrichment sequencing (RenSeq)³, an NLR exome-capture technique, we saw expression levels of full-length transcripts of *Sr22*, *Sr35*, *Sr45* and *Sr50* in each transgenic line that were similar to those from the equivalent endogenous wheat genes (Fig. 3a and Supplementary Figs. 12–15). Likewise, *Sr55* transgene expression in P19 and P52 was similar to that of the endogenous gene (<twofold different), although higher expression occurred in P60 (Fig. 3b). We then confirmed the functionality of *Sr35* and *Sr50* in each multi-transgene line using a protoplast assay⁸. Firstly, Fielder protoplasts were transformed with a luciferase reporter gene (*luc*) and combinations of the cloned *Sr35* (ref. 4) or *Sr50* (ref. 5) NLR genes and cloned *Pgt AvrSr50* (ref. 9) or *AvrSr35* (ref. 10) avirulence genes. Protoplasts expressing *Sr35* and *AvrSr35* or *Sr50* and *Avr50* had significantly reduced luciferase expression compared with those expressing each gene alone, indicative of resistance gene function (Fig. 3c,d). Having validated this protoplast assay, we then isolated protoplasts from homozygous seedlings of each multi-transgene line. Protoplasts from each line



had significantly reduced luciferase expression when transformed with either *AvrSr50* or *AvrSr35* compared with those transformed with a control GFP plasmid, demonstrating that *Sr50* and *Sr35* function in each line (Fig. 3e).

To test the function of *Sr55*, we established a field leaf rust nursery infected with three *Pt* races. Area under disease progress curve (AUDPC) values for lines carrying *Sr55* (multi-transgene, single transgene and nontransgenic) were significantly lower (one-sided ANOVA, $P < 0.05$) than those for either Fielder,



Thatcher or respective null siblings, with the exception of P52 and null P52 lines (Fig. 3f and Supplementary Table 4). Disease progression was intermediate for null segregants compared with that of Fielder, for unknown reasons. These data are consistent with *Sr55* providing characteristic partial APR to *Pt* in the multi-transgene lines.

During our experiments, a new *Pgt* isolate, IT76a/18 of race TTRTF, was detected in Sicily in 2017 (ref. ¹¹) with rare combined virulence for both *Sr35* and *Sr50*. We infected control and single-gene transgenic seedlings with IT76a/18 and confirmed its virulence toward *Sr35* and *Sr50*, but also *Sr45*, while avirulence toward *Sr22* was observed (Fig. 3g and Supplementary Table 6).

Fig. 3 | Expression and function of resistance genes in multi-transgene lines. **a**, cDNA sequences encoding NLR genes were enriched using RenSeq exome capture and deep sequenced. The percents of total sequencing reads (y axis) that mapped at high stringency to *Sr22*, *Sr35*, *Sr45* and *Sr50* are shown in each graph. Approximately 24 million reads were sequenced for each sample. Exact read numbers and alignments are shown in Supplementary Figs. 12–15. White columns labeled *Sr22*, *Sr35*, *Sr45* or *Sr50* represent samples from control homozygous nontransgenic wheat accessions that contain the endogenous gene indicated. RNA was isolated from a pooled T₁ family from each multi-transgene line for lines P19, P52 and P60 (black columns). Data shown are from a single experiment. **b**, Quantitative RT-PCR expression analysis of the *Sr55* gene in wheat seedlings. cDNA samples were amplified by PCR using primers that amplify transcripts from both the *Sr55* resistance gene (gray columns) and the equivalent D genome-encoded susceptibility allele, *sr55D* (white column), which differs from the former by only two nonsynonymous nucleotide substitutions. These amplification products were sequenced and normalized relative to an *sr55* homologue (*sr55-4A*) that was also coamplified by these primers and expressed in all lines. RNA was from a Thatcher line with *Sr55* (Tc55) that was homozygous for the endogenous *Sr55* gene (*Sr55D*^{+/+}; *sr55-4A*^{+/+}), Fielder (F) wheat (*sr55D*^{+/+}; *sr55-4A*^{+/+}) and homozygous T2 progeny (*Sr55* transgene^{+/+}; *sr55D*^{+/+}; *sr55-4A*^{+/+}) from each multi-transgene line (P19, P52, P60). Each column shows the mean normalized expression from three biological replicate experiments with each individual experimental value illustrated as a black dot on each column, and data are shown as mean ± s.d. Columns with the same letters above are not significantly different by one-sided ANOVA and post hoc Tukey tests ($P < 0.05$). All significantly different samples had $P = 0.001$, except for the following: Thatcher *Sr55* resistance allele versus the Fielder susceptible allele ($P = 0.002$), Thatcher *Sr55* resistance allele versus the P52 *Sr55* resistance allele ($P = 0.005$) and the P19 *Sr55* resistance allele versus the P52 susceptible allele ($P = 0.005$). Columns labeled 'c' were not significantly different from each other, with P values ranging from 0.504 to 0.899, while columns labeled 'b' had $P = 0.899$. **c–d**, Protoplasts were isolated from Fielder seedlings and transformed with a *Ubi-luciferase* construct (*luc*) and either *Ubi-Sr50*, *Ubi-AvrSr50* or both genes (*Sr+Avr*) (**c**) or *Ubi-Sr35*, *Ubi-AvrSr35* or both genes (*Sr+Avr*) (**d**). After transformation (24 h), protoplasts were assayed for luciferase activity. Luciferase activity was normalized against a protoplast control sample transformed with *Ubi-luciferase* and *Ubi-GFP*, with the latter acting as a DNA control plasmid only. A substantial reduction in luciferase activity was indicative of cell death. Pairwise two-sided *t*-tests showed a significant difference ($P < 0.05$) in luciferase activity only between protoplasts transformed with each resistance gene–avirulence gene pair when compared with single-gene controls (that is, *Sr50* versus both genes, $P = 0.042$; *AvrSr50* versus both genes, $P = 0.039$; *Sr50* versus *AvrSr50*, $P = 0.435$ (not significant); *Sr35* versus both genes, $P = 0.019$; *AvrSr35* versus both genes, $P = 9.51 \times 10^{-5}$; *Sr35* versus *AvrSr35*, $P = 0.055$ (not significant)). Columns show mean luciferase expression normalized to a GFP plasmid control, and these average values were derived from three biological replicates for the *Sr50* and *AvrSr50* analyses, while four biological replicates were performed for *Sr35* and *AvrSr35* experiments. Individual experimental values are shown as black dots on each column, with each experimental value (black dot) being the average of three technical replicates. Data are shown as mean ± s.d. **e**, Protoplast assays confirming *Sr35* and *Sr50* gene function. Protoplasts from homozygous multi-transgene lines P19, P52 and P60 were transformed with both a *Ubi-luciferase* construct (*luc*) and either *Pgt* avirulence gene *AvrSr35* or *AvrSr50*. After transformation (24 h), protoplasts were assessed for luciferase activity, and data were normalized against a protoplast control sample transformed with *Ubi-luciferase* and *Ubi-GFP*. A substantial reduction in luciferase activity was indicative of cell death. A statistically significant difference in luciferase activity was observed between the GFP control and protoplasts transformed with either *AvrSr35* or *AvrSr50* for each plant line (one-sided ANOVA with post hoc Tukey, comparing *Ubi-GFP* versus *AvrSr35*, $P = 0.001$ for P19, P52 and P60 and *GFP* versus *AvrSr50*, $P = 0.001$ for P19, P52 and P60). Columns show the average of four biological replicates with three technical replicates per experiment. Data are shown as mean ± s.d. Each individual experimental value is shown as a black dot on the column. **f**, AUDPC of *Pt* on homozygous T₂ progeny of multi-transgene lines (P19, P52, P60), their null control lines (null P60, null P52), Fielder lines and a Fielder transgenic line containing only the *Sr55* gene (*Sr55-2*). Also shown are wheat cultivar Thatcher (Tc) and a near-isogenic Thatcher line containing *Sr55* (Tc + *Sr55*). Each column is the mean AUDPC calculated for each genotype from four replicate plots. AUDPC values for individual plots are shown as black dots on each column. Data are shown as mean ± s.d. Significantly (one-sided ANOVA, $P < 0.05$) less *Pt* growth occurred on P60, P19, *Sr55-2* and Tc + *Sr55* lines compared with that on their controls (null P60, Fielder and Tc, respectively). *Pt* growth on line P52-1 was not significantly different from that on the null P52 line. Statistical analyses are shown in Supplementary Table 4. **g**, Infection of wheat seedlings with Italian isolate IT76a/18 of *Pgt* race TTRTF. T₂ seedling leaves derived from homozygous T₁ lines of multi-transgene lines P19, P52 and P60 are labeled in red (numbers preceded with a hyphen on T₂ transgenic leaf labels designate the T₁ parent of origin). Null-segregant T₂ seedlings of multi-transgene lines are shown with blue labels. Seedling leaves from homozygous transgenic Fielder plants that contain the single resistance transgene indicated are labeled in purple. Leaves from nontransgenic wheat lines are labeled in green with the endogenous *Pgt* resistance gene indicated. Photographs were taken 18 d after inoculation with *Pgt*. Four seedlings of each genotype were infected in two replicate experiments.

Seedlings of each multi-transgene line were also highly resistant to IT76a/18, thereby demonstrating the function of *Sr22* in each line (Fig. 3g and Supplementary Table 6). Collectively, our data provide biological evidence that *Sr22*, *Sr35*, *Sr50* and *Sr55* function in each multi-transgene line. We were unable to confirm *Sr45* function due to lack of a suitable discriminatory rust isolate or a cloned *AvrSr45* effector, although *Sr45* RNA expression levels similar to those of wild type occurred in multi-transgene lines (Fig. 3a).

These data show that we have introduced five different *Pgt* resistance genes into three independent wheat lines as a multi-transgene cassette and full-length copies of these genes have co-integrated into a single Mendelian locus in each line. These loci confer high levels of resistance to *Pgt* and partial resistance to *Pt*, with biological function confirmed for four genes in this five-gene stack. In a similar strategy with potato plants, three ASR genes were combined that each provided isolate-specific resistance to the potato late blight pathogen *Phytophthora infestans*, although single-locus inheritance of these events was not demonstrated^{12–14}. This gene-stacking approach is particularly amenable for resistance genes cloned from sexually incompatible relatives and/or associated with deleterious

linkage drag to increase the available resistance gene pool. Gene stacks will also greatly simplify responsible and durable deployment of these valuable genetic resources by reducing single-gene deployment. Our study also reaffirms the value of cloned *Pgt* effectors in verifying resistance gene function, as future stacks will ideally use nondeployed genes for which known pathogen virulence is not apparent.

Deployment of multi-transgene loci to increase resistance durability has the potential to become routine in the future with improving transformation¹⁵ and cloning technologies^{3,16}. However, the recent emergence of *Pgt* isolate IT76a/18 (race TTRTF), which overcame three of the four ASR genes in our stack, provides a cautionary tale. Deployment of our multi-transgenic lines in regions containing isolate IT76a/18, such as Europe, would be effectively equivalent to single-gene deployment of *Sr22*, albeit in combination with the *Sr55* APR gene, making selection of pathogen virulence for *Sr22* likely and thereby negating the value of this gene stack. In contrast, *Sr22*, *Sr35*, *Sr45*, *Sr50* and *Sr55* remain effective against the *Pgt* Ug99 lineage^{4,17}, making deployment of this resistance gene stack potentially very valuable in Africa and the Middle East. Similarly,

the *Sr22*, *Sr35*, *Sr50* and *Sr55* genes remain effective against most *Pgt* isolates in North America^{3–5,18}.

Strategic deployment therefore appears necessary for maximum benefit of gene stacks. Several strategies can be envisaged for future deployment. Gene stacks containing ASR genes could be tailored to target regional pathogen populations rather than global ones. While exotic incursions of new *Pgt* isolates do occur, they are relatively rare compared with local adaptation. For example, it has been over 20 years since the widely virulent African Ug99 lineage emerged, but it has not yet appeared in Europe, USA, Canada, India, China or Australia¹⁷. Potentially, regionally effective gene stacks could be periodically cycled to enhance durability by alternating the multi-resistance selection against the pathogen population.

Another approach would be to use two separate gene stacks to increase the number of effective resistance genes in a single cultivar with only a modest increase in breeding effort required. One gene-stack combination is unlikely to have enough effective ASR gene redundancy to provide durable resistance to all *Pgt* pathogen populations globally, unless more very broadly effective genes, like *Sr26* and *Sr61*, can be found. At this point, we do not know what the upper size limit is for a single-gene stack. We have produced a 63-kb eight-gene stack but have not yet introduced it into wheat.

In contrast to ASR genes, some APR genes, which provide partial resistance only, can be broadly effective and show resistance additivity¹⁷. A gene stack of additive APR genes has the potential for global use. However, APR genes can show different efficacy in different genetic backgrounds under high disease pressure, which is another reason for strategic tailoring of gene stacks. APR gene combinations that provide good levels of protection in locally adapted genetic backgrounds will be required.

The gene-stacking advances we present here, coupled with the recent development of highly efficient *Agrobacterium* transformation of wheat that is less genotype-dependent^{19,20}, suggest that deploying regionally targeted stacks in locally adapted cultivars is feasible. This approach mimics current breeding strategies, which produce locally adapted cultivars with resistance primarily against local *Pgt* races, although some pre-emptive breeding is included. Therefore, while multi-transgene stacks may not be immune to pathogen virulence evolution, they represent a valuable additional weapon for disease protection by simplifying breeding efforts and increasing durability when strategically deployed.

Online content

Any methods, additional references, Nature Research reporting summaries, source data, extended data, supplementary information, acknowledgements, peer review information; details of author contributions and competing interests; and statements of data and code availability are available at <https://doi.org/10.1038/s41587-020-00770-x>.

Received: 25 October 2019; Accepted: 12 November 2020;
Published online: 4 January 2021

References

- Lewis, C. M. et al. Potential for re-emergence of wheat stem rust in the United Kingdom. *Commun. Biol.* **1**, 13 (2018).
- Periyannan, S., Milne, R. J., Figueroa, M., Lagudah, E. S. & Dodds, P. N. An overview of genetic rust resistance: from broad to specific mechanisms. *PLoS Pathog.* **13**, e1006380 (2017).
- Steuernagel, B. et al. Rapid cloning of disease-resistance genes in plants using mutagenesis and sequence capture. *Nat. Biotechnol.* **34**, 652–655 (2016).
- Saintenac, C. et al. Identification of wheat gene *Sr35* that confers resistance to Ug99 stem rust race group. *Science* **341**, 783–786 (2013).
- Mago, R. et al. The wheat *Sr50* gene reveals rich diversity at a cereal disease resistance locus. *Nat. Plants* **1**, 15186 (2015).
- Schafer, J. F. & Roelfs, A. P. Estimated relationship between numbers of urediniospores of *Puccinia graminis* f. sp. *tritici* and rates of occurrence of virulence. *Phytopathology* **75**, 749–750 (1985).
- Moore, J. W. et al. Recent evolution of a hexose transporter variant confers resistance to multiple pathogens in wheat. *Nat. Genet.* **47**, 1494–1498 (2015).
- Arndell, T. et al. gRNA validation for wheat genome editing with the CRISPR-Cas9 system. *BMC Biotechnol.* **19**, 71 (2019).
- Chen, J. et al. Loss of *AvrSr50* by somatic exchange in stem rust leads to virulence for *Sr50* resistance in wheat. *Science* **358**, 1607–1610 (2017).
- Salcedo, A. et al. Variation in the *AvrSr35* gene determines *Sr35* resistance against wheat stem rust race Ug99. *Science* **358**, 1604–1606 (2017).
- Bhattacharaya, S. Deadly new wheat disease threatens Europe's crops. *Nature* **542**, 145–146 (2017).
- Zhu, S., Li, Y., Vossen, J. H., Visser, R. G. F. & Jacobsen, E. Functional stacking of three resistance genes against *Phytophthora infestans* in potato. *Transgenic Res.* **21**, 89–99 (2012).
- Haesaert, G. et al. Transformation of the potato variety Desiree with single or multiple resistance genes increases resistance to late blight under field conditions. *Crop Prot.* **77**, 163–175 (2015).
- Ghislain, M. et al. Stacking three blight resistance genes from wild species directly into African highland potato varieties confers complete field resistance to local blight races. *Plant Biotechnol. J.* **17**, 1119–1129 (2019).
- Lowe, K. et al. Morphogenic regulators Baby boom and Wuschel improve monocot transformation. *Plant Cell* **28**, 1998–2015 (2016).
- Arora, S. et al. Resistance gene discovery and cloning by sequence capture and association genetics. *Nat. Biotechnology* **37**, 139–143 (2019).
- Singh, R. P. et al. Emergence and spread of new races of wheat stem rust: continued threats to food security and prospects of genetic control. *Phytopathology* **105**, 872–874 (2015).
- Borlaug Global Rust Initiative. Knowledge Center—Resistance Genes. <https://bgri.cornell.edu/knowledge-center> (accessed 30 November 2020).
- Ishida, Y., Tsunashima, M., Hiei, Y. & Komari, T. Wheat (*Triticum aestivum* L.) transformation using immature embryos. in *Methods in Molecular Biology, Agrobacterium Protocols*, 3rd edn. (ed. Wang, K.) (Springer, 2014).
- Richardson, T., Thistleton, J., Higgins, T. J., Howitt, C. & Ayliffe, M. Efficient *Agrobacterium* transformation of elite wheat germplasm without selection. *Plant Cell, Tissue Organ Cult.* **119**, 647–659 (2014).

Publisher's note Springer Nature remains neutral with regard to jurisdictional claims in published maps and institutional affiliations.

© The Author(s), under exclusive licence to Springer Nature America, Inc. 2021

Methods

Rust phenotyping at the seedling stage in the greenhouse. The resistance spectrum of multi-transgene wheat lines was assessed at the University of Minnesota using a diverse panel of virulent *Pgt* isolates (Supplementary Table 3). Race TTTTF (isolate 02MN84A-1-2) is one of the most widely virulent races reported from the United States; Minnesota race QTHJC (69MN399) is virulent toward Fielder plants and was therefore used in field tests; Kenyan isolate 04KEN156/04 (that is, race TTKSK) has the same virulence pattern as the original Ugandan Ug99 isolate with virulence toward lines with *Sr31*. Ethiopian isolate 13ETH18-1 caused a major epidemic in Ethiopia on wheat cultivar Digalu and keys to race TKTF. Two TRTF races were used, Georgian isolate 14GEO189-1 and Italian isolate ITSN18, with the former being virulent for lines with *Sr50* and the latter being avirulent for lines with *Sr50*. Yemen race JRCQC (09ETH80-3) has a unique virulence pattern. Stem rust evaluations with foreign isolates were conducted in a Biosafety Level 3 Containment Facility, while tests with domestic isolates were performed in a greenhouse as previously described²¹. Rust ITs were scored 12–14 d post-plant inoculation on a scale of 0 to 4 (ref. ²²), where IT 0 represents extreme resistance and IT 4 represents full susceptibility. Three seedlings of each plant genotype were infected with each rust isolate. A completely randomized design was used for each experiment and was repeated twice. Susceptible wheat controls McNair 701 (Citr 15288), Morocco (PI 431591) or Thatcher (PI 10003) were included in each experiment as a positive control. Rust evaluations to assess *Sr22* gene function in seedlings of multi-transgene lines were performed at Aarhus University, Denmark, using the recently described Sicilian *Pgt* isolate IT76a/18 (TRTF), which has virulence for *Sr35* and *Sr50* lines and, as shown in this study, virulence for lines with *Sr45* as well. *Sr22*, *Sr35*, *Sr45* and *Sr50* provide ASR to *Pgt* only, whereas *Sr55* provides APR to all three wheat rust diseases. To confirm that the seedling-stage resistance observed in multi-transgene lines was *Pgt*-specific, seedlings were also challenged with *Pt* and *Pst* isolates using the seedling assays described above (Supplementary Table 3).

Stem rust phenotyping at the adult plant stage in the field. Homozygous T₁ families from multi-transgene lines, Fielder transgenic lines containing a single transgene and control lines were planted at the University of Minnesota Rosemount Research and Outreach Center in Rosemount, MN in 2018 and 2019. A completely randomized design was used with three replicates per genotype in 2018 and four replicates in 2019. Approximately 25 seeds per line were planted in each plot. Wheat cultivars Fielder, Morocco and LMPG-6 were used as susceptible controls. *Pgt* race QTHJC was selected, because it is a Minnesotan isolate with virulence for wild-type Fielder plants. When the first nodes of plants were detectable (Zadoks 31 (ref. ²³)), they were inoculated with a suspension of *Pgt* urediniospores (1 g urediniospores per 1 L Soltrol 170 mineral oil; Phillips Petroleum) using an ultra-low volume sprayer (Mini-ULVA, Micron Group). Three additional inoculations were made in successive weeks to ensure high infection levels during the later stages of crop development. The percentage (0–100% scale) of stem and leaf sheath tissue covered by uredinia was assessed using the modified Cobb scale²⁴ from the late-milk-to-late-dough stages (Zadoks 77 to 85 (ref. ²³)) of crop development. Terminal rust severity was used for statistical analysis of data, which was the average of replicate plots. Lines were also assessed for adult plant infection responses (IRs) using the scale of R, resistant (minute-to-small uredinia surrounded by chlorosis or necrosis); MR, moderately resistant (medium-sized uredinia often surrounded by chlorosis); MS, moderately susceptible (medium-to-large erumpent uredinia with little or no chlorosis); and S, susceptible (very large erumpent uredinia with little or no chlorosis)²⁵. An additional category of HR (highly resistant) was added to accommodate cases in which clear hypersensitive infection sites were present but with no pathogen sporulation.

Leaf rust phenotyping at the adult plant stage in the field. Natural *Pt* inoculum infected the leaves of wheat plants in the 2018 field nursery. Because lines with *Sr55* are effective against the leaf rust pathogen in adult plants, notes on rust severity and IRs were recorded in 2018 at mid-to-hard-dough developmental stages (Zadoks 83 to 87 (ref. ²³)) as described above for stem rust. *Pt* isolates were recovered from the nursery and assayed for their virulence phenotypes on wheat leaf rust differentials²⁶. Three leaf rust races common to the USA northern Great Plains were detected, MNPSD, MBDS and MPPSD. To more thoroughly investigate the preliminary results obtained in 2018, a separate inoculated leaf rust nursery at Rosemount was established in 2019, using methods described above for stem rust and four replicates per genotype. Susceptible cultivar Thatcher (PI 10003) was planted around the perimeter of the nursery and used as 'spreader' plants to enable developing leaf rust to spread naturally onto the test entries. Thatcher plants were inoculated three times: first by needle injection of a urediniospore suspension (250 mg urediniospore composite of races MNPSD, MBDS and MPPSD in equal proportions in 0.25 L distilled water and 2 ml Tween-20) into the stems of plants when the first node was detectable (Zadoks 31 (ref. ²³)) and then twice by foliar spray in successive weeks as described above for stem rust. In 2019, notes on rust severity and IRs were recorded on four different dates during the season. For assessing the partial APR to *Pt* conferred by *Sr55*, severity data for the four scoring dates were used to calculate an AUDPC. Transgenic lines P60 and P19 were compared to null sibling segregants by one-sided ANOVA and post hoc Dunnett

test. P19 and *Sr55*-2 lines were compared with the Fielder control, while Thatcher was compared with a near-isogenic line containing *Sr55*.

Assessment for possible pleiotrophic effects on the growth and development of multigene transgenic lines. A greenhouse experiment was performed to determine whether expression of the multigene cassette caused any detrimental pleiotrophic effects on vegetative growth and reproductive development. Eight lines were included in the experiment: Fielder wild type, two null-segregant siblings (null P52 and null P60) and five multi-transgene lines (P60-22, P60-10, P19-12, P19-10 and P52-1). Plants were grown in square plastic pots (10 × 10 cm) containing a 50:50 mix of commercial potting soil (Sun Gro Professional Growing Mix, Sun Gro Horticulture) and steam-sterilized native soil. Slow-release fertilizer (Osmocote 14-14-14, Scott's Company) was applied at planting. A completely randomized design with 20 replicates per line was used in the experiment. Plants were grown at day and night temperatures of 25 °C and 14 °C, respectively, with 400-W high-pressure sodium lamps providing supplemental light (300 μmol p s⁻¹ m⁻²) for a 16-h photoperiod and watered daily and fertilized biweekly with a water-soluble formulation (Jack's General Purpose 20-10-20, JR Peters). The growth stage of each plant was assessed biweekly using the Zadoks scale²³. When the first spike of each plant emerged fully, the length and width of flag and penultimate (flag-1) leaves were measured and used to calculate leaf area. Plant height was recorded at maturity as the length from the crown to the top of the spike, excluding awns. The total number of tillers were recorded for each plant. Seed number and seed size were determined using a MARViN digital seed analyzer (MARViTECH). Total seed weight and 1,000 grain weight were measured for each plant.

Production of multi-transgene vectors. Two donor vectors (pDONOR1 and pDONOR2) were produced using plasmid pBR322 as a backbone (Supplementary Fig. 1a). The pDONOR1 vector encodes a *lacZ* reporter gene flanked by *attL1* and *attP1* Gateway recombination sites in juxtaposition to a β-lactamase ampicillin resistance gene, followed by a multiple cloning site flanked by *attR3* and *attL2* sites in which resistance genes of interest were cloned. A *loxP* Cre recombinase site was located between *attR3* and the ampicillin resistance gene (Supplementary Fig. 1b). The pDONOR2 vector differed from pDONOR1 only in that *attL2* was replaced with *attL3*, and the *attR3* site was replaced with *attR2* (Supplementary Fig. 1c). The binary vector pYL-TAC380H, kindly supplied by Y.G. Liu (South China Agricultural University, China)²⁷, was used as the backbone for a destination vector after the addition of a β-lactamase ampicillin resistance gene flanked by *attR1* and *attR2* into the T-DNA region of this plasmid (inserted as a BamHI- and BstXI-digested fragment into the BamHI and I-SceI sites of pYL-TAC380H) to create the binary plasmid p380HH (Supplementary Fig. 1a). The p380HH vector encodes a hygromycin-selectable marker gene for plant transformation. The *Sr22* resistance gene in pDONOR1 was inserted into p380HH using LR Gateway recombination (Gateway LR Clonase II Enzyme mix, Thermo Fisher) (Supplementary Fig. 1b). Following this reaction, the sample was digested with the restriction enzyme I-SceI, which cleaves only pDONOR1 and non-recombined p380HH vector. After transforming the digested recombinase sample into *E. coli* strain H10β, positive colonies were identified as blue colonies that expressed *lacZ*. Plasmid DNA was isolated from an *Sr22*/p380HH-containing colony and subjected to BP recombination (Gateway BP Clonase II Enzyme mix, Thermo Fisher), which removed *lacZ* and regenerated an *attR1* site (Supplementary Fig. 1b). The *Sr35* gene in donor vector D2 was then incorporated into p380HH + *Sr22*- Δ *lacZ*, again by LR Gateway recombination followed by digestion with PI-SceI and positive *lacZ* selection (Supplementary Fig. 1c). Removal of *lacZ* and *attR1* regeneration was again achieved by BP recombination (Supplementary Fig. 1c). Sequential reiteration of this cloning strategy was used to insert the *Sr50*, *Sr55* and *Sr45* sequences from pDONOR1 and pDONOR2, respectively. The last remaining *lacZ* and donor vector sequence were removed using Cre recombinase (Supplementary Fig. 1d) to generate the final *Sr45*/*Sr55*/*Sr35*/*Sr22*/p380HH binary vector sequence. Each resistance gene was expressed using endogenous regulatory sequences, being flanked by approximately 2 kb of 5' sequence and 1 kb of 3' sequence and including all native introns.

Wheat transformation and molecular analysis. Scutellum tissue from wheat cultivar Fielder was transformed with *Agrobacterium* strain GV3101, using hygromycin for selection as previously described^{19,20}. DNA was isolated using CTAB extraction and DNA was transferred to Biodyne nylon membranes (Pal Corp.) for DNA blot analysis. DNA probes were labeled by random hexamer priming using ³²P-labeled dCTP. For PCR analysis, 100 ng of genomic DNA template was amplified using Phire Hot Start II DNA Polymerase (Thermo Fisher Scientific). In each DNA blot figure, all samples were colocalized on the same membrane, and DNA blot images are presented in full in Supplementary Fig. 16. The lanes were cut in some instances to remove other intervening samples on the blot that were not relevant to the data presented, or in some cases were obscured by background. DNA primer sequences and probe sequences are shown in Supplementary Table 7.

***Sr55* expression analysis.** Expression of the *Sr55* transgene was quantified by RT-PCR and amplicon deep sequencing. RNA was extracted from pooled leaf

tissue of eight homozygous seedlings for each genotype, and cDNA was produced using a SuperScript III Reverse Transcriptase kit (Invitrogen). cDNA samples were PCR amplified with primers that amplified products from both the *Sr55* gene and the equivalent susceptibility allele, *sr55*, which differs from the former by only two nonsynonymous nucleotide substitutions. These primers also amplified transcripts from an *sr55* homoeologue located on chromosome 4A (*sr55-4A*). The *sr55-4A* sequence was used to normalize the expression of the D genome-encoded endogenous *Sr55* gene in a Thatcher control line with *Sr55*; the *sr55D* susceptibility allele was present in both transgenic and nontransgenic Fielder lines, and the *Sr55* transgene was present in multi-transgene lines. After 21 thermal cycles, amplification products were sequenced by Illumina (a minimum of 27,000 MiSeq 250-bp paired-end reads per sample), and reads from each sample were aligned to the *Sr55*, *sr55D* and *sr55-4A* genes using CLC Genomics Workbench (Qiagen). *Sr55* and *sr55D* reads were then normalized relative to the number of *sr55-4A* reads present in each sample. Adaptor sequences were included in *Sr55* primers used for PCR amplification (Supplementary Table 7). Three biological replicate experiments were performed using homozygous seedlings.

Protoplast assays. Protoplasts were isolated from homozygous multi-transgene lines and Fielder lines using 9-d-old seedlings that had been grown under low light⁸. ORFs for *Pgt* avirulence genes *AvrSr50* and *AvrSr35* were cloned under the regulatory control of a maize polyubiquitin (*Ubi*) promoter and the 3' termination sequence from the *Agrobacterium* tumor morphology 1 gene and the cauliflower mosaic virus 35S terminator, respectively. Similarly, an *Sr50* cDNA sequence and the *Sr35* coding sequence, including introns, were cloned under the regulatory control of the above *Ubi* and 35S terminator sequences. DNA was prepared using a Qiagen Maxiprep kit, and protoplasts were transformed with 40% polyethylene glycol. Fielder protoplast samples were cotransformed with *Ubi*-luciferase and either *Ubi-AvrSr50*, *Ubi-AvrSr35*, *Ubi-Sr50*, *Ubi-Sr35* or *Ubi*-GFP. The *Ubi-Sr50* and *Ubi-Sr35* genes were not cotransformed into protoplasts derived from multi-transgene lines, as these two transgenes were already present in these plants, albeit under the regulatory control of their endogenous promoters. After 24 h, post-transformation luciferase activity was quantified using a commercial luciferase assay system (Promega) and a FLUOstar Omega microplate reader (BMG LABTECH). All samples were normalized relative to the luciferase expression of protoplasts cotransformed with *Ubi*-luciferase and *Ubi*-GFP control plasmids. Each graph in Fig. 3c,d,e shows combined data from three or four biological replicates with three technical replicates per experiment.

RenSeq expression analysis. RNA was extracted from pooled tissue of segregating T₁ seedlings (equivalent to hemizygous expression) derived from T₀ multi-transgene lines P19, P52 and P60. Transgene expression was compared with expression in control wheat lines Schomburgk, J36-16, 5406 and Gabo, which contain endogenous *Sr22*, *Sr35*, *Sr45* and *Sr50* genes, respectively. RNA was extracted from seedlings at the fourth leaf stage, and cDNA was produced using a SuperScript III Reverse Transcriptase kit (Invitrogen). DNA adaptors were added to cDNA, and NLR sequences were enriched and sequenced by Arbor Biosciences using RenSeq exome capture and an improved version of the previously published Triticeae bait library, available at <https://github.com/steuernb/MutantHunter>²⁸, and HiSeq 2500 paired-end sequencing. cDNA sequence reads were then aligned against transgene-coding sequences using CLC Genomics Workbench (Qiagen) with default parameters and using 100% similarity and 95% sequence length. Twenty-four million reads per sample were aligned to reference NLR sequences, and matching reads were quantified (Supplementary Figs. 12–15).

Statistical analyses. For statistical analyses, R version 3.6.0 (2019-04-26) with R Studio and the following packages were used: Tidyverse (<https://cran.r-project.org/web/packages/tidyverse/index.html>) for data manipulation and DescTools (<https://cran.r-project.org/web/packages/DescTools/index.html>) for Dunnett's tests. Agricolae (<https://cran.r-project.org/web/packages/agricolae/index.html>) was used to calculate AUDPC for the 2019 leaf rust data. AUDPC values were then further analyzed statistically. ANOVA analyses (one-sided) were conducted for a variable of interest (that is, AUDPC, terminal severity, plant height), and if ANOVA yielded $P < 0.05$, a Dunnett test was used to determine which groups were significantly

different from a given control. For comparing Thatcher and Thatcher with *Sr55*, a Student's *t*-test was used.

Reporting Summary. Further information on research design is available in the Nature Research Reporting Summary linked to this article.

Data availability

See the Nature Research Reporting Summary. All raw data presented in Fig. 3a, Supplementary Figs. 12–15 (RenSeq sequence data) and Fig. 3b (*Sr55* quantitative expression sequencing data) were deposited at NCBI under Bioproject accession no. PRJNA624003. The following DNA sequences were also deposited at NCBI, that is, the *Sr45-Sr55-Sr50-Sr35-Sr22* T-DNA sequence (GenBank accession no. MT165900), the p380HH vector (region from *attR1* to *attR2*; GenBank accession no. MT180324), the pDONOR1 (D1) vector (GenBank accession no. MT180325) and the pDONOR2 (D2) vector (GenBank accession no. MT180326).

References

- Huang, S., Steffenson, B. J., Sela, H. & Stinebaugh, K. Resistance of *Aegilops longissima* to the rusts of wheat. *Plant Dis.* **102**, 1224–1235 (2018).
- Stakman, E. C., Stewart, D. M. & Loegering, Q. W. *Identification of Physiologic Races of Puccinia graminis var. tritici* (Department of Agriculture, Agricultural Research Service, 1962).
- Zadoks, J. C., Chang, T. T. & Konzak, C. F. A decimal code for the growth stages of cereals. *Weed Res.* **14**, 415–421 (1974).
- Peterson, R., Campbell, A. & Hannah, A. A diagrammatic scale for estimating rust intensity on leaves and stems of cereals. *Can. J. Res.* **26C**, 496–500 (1948).
- Roelfs, A. P., Singh, R. P. & Saari, E. E. *Rust Diseases of Wheat: Concepts and Methods of Disease Management* (CIMMYT, 1992).
- Long, D. L. & Kolmer, J. A. A North American system of nomenclature for *Puccinia triticina*. *Phytopathology* **79**, 525–529 (1989).
- Zhu, Q. et al. Development of 'purple endosperm rice' by engineering anthocyanin biosynthesis in the endosperm with a high-efficiency transgene stacking System. *Mol. Plant* **10**, 918–929 (2017).
- Marchal, C. et al. BED-domain-containing immune receptors confer diverse resistance spectra to yellow rust. *Nat. Plants* **4**, 662–668 (2018).

Acknowledgements

We thank the 2Blades Foundation for financial support, Y.G. Liu for the 380H vector and C. Chen for assistance with figures.

Author contributions

Experimental design: M.A., M.L., B.J.S., T.L.R., R.F.; manuscript preparation: M.A., M.L., B.J.S., T.L.R., R.F., B.B.H.W.; field trials and pathology assays: B.J.S., M.J., O.M., J.A.K., M.P., C.S.; protoplast assays: M.L., A.W., D.O., P.D.; molecular analysis: S.C., A.W., M.L., M.H.; construct production: M.L., L.X., A.W., S.C., B.S., B.B.H.W., R.M., S.P., E.L.; bioinformatics: N.M.U., B.S., M.L.; wheat transformation: T.R., D.B., M.A.

Competing interests

T.L.R. was employed by the 2Blades Foundation, while R.F. is chairman of the 2Blades board. Both were involved in the conceptualization, design, analysis and preparation of this research manuscript. The 2Blades Foundation cofunded the research presented.

Additional information

Supplementary information is available for this paper at <https://doi.org/10.1038/s41587-020-00770-x>.

Correspondence and requests for materials should be addressed to M.A.

Peer review information *Nature Biotechnology* thanks the anonymous reviewers for their contribution to the peer review of this work.

Reprints and permissions information is available at www.nature.com/reprints.

Reporting Summary

Nature Research wishes to improve the reproducibility of the work that we publish. This form provides structure for consistency and transparency in reporting. For further information on Nature Research policies, see [Authors & Referees](#) and the [Editorial Policy Checklist](#).

Statistics

For all statistical analyses, confirm that the following items are present in the figure legend, table legend, main text, or Methods section.

- | | |
|-------------------------------------|--|
| n/a | Confirmed |
| <input type="checkbox"/> | <input checked="" type="checkbox"/> The exact sample size (n) for each experimental group/condition, given as a discrete number and unit of measurement |
| <input type="checkbox"/> | <input checked="" type="checkbox"/> A statement on whether measurements were taken from distinct samples or whether the same sample was measured repeatedly |
| <input type="checkbox"/> | <input checked="" type="checkbox"/> The statistical test(s) used AND whether they are one- or two-sided
<i>Only common tests should be described solely by name; describe more complex techniques in the Methods section.</i> |
| <input type="checkbox"/> | <input checked="" type="checkbox"/> A description of all covariates tested |
| <input type="checkbox"/> | <input checked="" type="checkbox"/> A description of any assumptions or corrections, such as tests of normality and adjustment for multiple comparisons |
| <input type="checkbox"/> | <input checked="" type="checkbox"/> A full description of the statistical parameters including central tendency (e.g. means) or other basic estimates (e.g. regression coefficient) AND variation (e.g. standard deviation) or associated estimates of uncertainty (e.g. confidence intervals) |
| <input type="checkbox"/> | <input checked="" type="checkbox"/> For null hypothesis testing, the test statistic (e.g. F , t , r) with confidence intervals, effect sizes, degrees of freedom and P value noted
<i>Give P values as exact values whenever suitable.</i> |
| <input checked="" type="checkbox"/> | <input type="checkbox"/> For Bayesian analysis, information on the choice of priors and Markov chain Monte Carlo settings |
| <input checked="" type="checkbox"/> | <input type="checkbox"/> For hierarchical and complex designs, identification of the appropriate level for tests and full reporting of outcomes |
| <input checked="" type="checkbox"/> | <input type="checkbox"/> Estimates of effect sizes (e.g. Cohen's d , Pearson's r), indicating how they were calculated |

Our web collection on [statistics for biologists](#) contains articles on many of the points above.

Software and code

Policy information about [availability of computer code](#)

- | | |
|-----------------|--|
| Data collection | <i>Provide a description of all commercial, open source and custom code used to collect the data in this study, specifying the version used OR state that no software was used</i> |
| Data analysis | For statistical analysis R version 3.6.0 (2019-04-26) with R Studio was used and the following packages; Tidyverse (https://cran.r-project.org/web/packages/tidyverse/index.html) for data manipulation and DescTools (https://cran.r-project.org/web/packages/DescTools/index.html) for Dunnett's Tests. Agricolae (https://cran.r-project.org/web/packages/agricolae/index.html) was used to calculate AUDPC for the 2019 leaf rust data. |

For manuscripts utilizing custom algorithms or software that are central to the research but not yet described in published literature, software must be made available to editors/reviewers. We strongly encourage code deposition in a community repository (e.g. GitHub). See the Nature Research [guidelines for submitting code & software](#) for further information.

Data

Policy information about [availability of data](#)

All manuscripts must include a [data availability statement](#). This statement should provide the following information, where applicable:

- Accession codes, unique identifiers, or web links for publicly available datasets
- A list of figures that have associated raw data
- A description of any restrictions on data availability

Data availability

Seven supplemental tables and 16 supplemental figures have been provided. All the raw data presented in Figure 3a, Figure S12-S15 (Renseq sequence data) and Figure 3b (Sr55 quantitative expression sequencing data) has been deposited at NCBI under Bioproject PRJNA624003.

The following DNA sequences have also been deposited at NCBI i.e.

Sr45/Sr55/Sr50/Sr35/Sr22 T-DNA sequence Genbank Accession MT165900
p380HH vector attR1 to attR2region Genbank Accession MT180324

pDONOR1 (D1) vector
pDONOR2 (D2) vector

Genbank Accession MT180325
Genbank Accession MT180326

Field-specific reporting

Please select the one below that is the best fit for your research. If you are not sure, read the appropriate sections before making your selection.

Life sciences Behavioural & social sciences Ecological, evolutionary & environmental sciences

For a reference copy of the document with all sections, see [nature.com/documents/nr-reporting-summary-flat.pdf](https://www.nature.com/documents/nr-reporting-summary-flat.pdf)

Life sciences study design

All studies must disclose on these points even when the disclosure is negative.

- Sample size Samples sizes were not calculated but are consistent with standard field trial, pathology assays and molecular biology assays.
- Data exclusions No data was excluded.
- Replication All attempts at replication were successful.
- Randomization Field trial and glasshouse rust inoculation experiments were randomized as described in the manuscript
- Blinding Blinding was not used through due to the large number of samples assessed in field trials and pathology assays. However, randomised replicate samples were used throughout.

Reporting for specific materials, systems and methods

We require information from authors about some types of materials, experimental systems and methods used in many studies. Here, indicate whether each material, system or method listed is relevant to your study. If you are not sure if a list item applies to your research, read the appropriate section before selecting a response.

Materials & experimental systems

- | n/a | Involvement in the study |
|-------------------------------------|--|
| <input checked="" type="checkbox"/> | <input type="checkbox"/> Antibodies |
| <input checked="" type="checkbox"/> | <input type="checkbox"/> Eukaryotic cell lines |
| <input checked="" type="checkbox"/> | <input type="checkbox"/> Palaeontology |
| <input checked="" type="checkbox"/> | <input type="checkbox"/> Animals and other organisms |
| <input checked="" type="checkbox"/> | <input type="checkbox"/> Human research participants |
| <input checked="" type="checkbox"/> | <input type="checkbox"/> Clinical data |

Methods

- | n/a | Involvement in the study |
|-------------------------------------|---|
| <input checked="" type="checkbox"/> | <input type="checkbox"/> ChIP-seq |
| <input checked="" type="checkbox"/> | <input type="checkbox"/> Flow cytometry |
| <input checked="" type="checkbox"/> | <input type="checkbox"/> MRI-based neuroimaging |